Theory of colossal magnetoresistance in manganites

1999 J. Phys.: Condens. Matter 11 4539

(http://iopscience.iop.org/0953-8984/11/23/308)

J. Phys.: Condens. Matter **11** (1999) 4539–4555. Printed in the UK PII: S0953-8984(99)98321-2

Theory of colossal magnetoresistance in manganites

C M Srivastava

Department of Physics, IIT, Powai, Mumbai 400 076, India

Received 13 October 1998

Abstract. The recent attempt to account for the existence of several magnetic phases in insulating perovskite manganites in terms of the interplay between the orbital and spin orders produced by the localized e_g and t_{2g} electrons is extended to the metallic state which is obtained on doping. It is shown that the activation energy for electrical conductivity obtained on the basis of the correlated polaron transport depends on the product of the spin and bond order parameters which changes rapidly near the magnetic transition temperature and accounts for the existence of colossal magnetoresistance in this system.

1. Introduction

The origin of the colossal magnetoresistance (CMR) in the perovskite manganites $A_{1-x}B_xMnO_3$ (A = La, Pr, Nd, Sm; B = Ca, Sr, Ba) remains unclear despite extensive effort [1–4]. Recently the electronic structure of manganites has been investigated and the effective Hamiltonian has been obtained taking into account the degeneracy of the e_g orbitals and strong electron correlations [5, 6]. It has been shown that in the mean-field approximation stable spin and orbital ordered phases exist and account for the stabilization of the low-symmetry A-type antiferromagnetic (AF) phase in $LaMnO_3$ due to the dependence of the magnetic interaction on the bond direction. The spin-wave spectrum derived for this model is consistent with a recent neutron scattering experiment on $LaMnO_3$ [5]. Furthermore, it has been shown that the origin of several magnetic phases observed in manganites lies in the interplay between the spin and orbital degrees of freedom. Wollan and Koehler [7] have carried out neutron diffraction studies of the spin structures as the concentration of Mn^{4+} in $La_{1-x}Ca_xMnO_3$ is varied. Goodenough [8] has given a qualitative theory of magnetic exchange via covalent bonds which explains the whole variety of ferromagnetic and AF spin structures observed in this system. In the theory of 'double' exchange [9–11] the magnetic order is a result of competition between super-exchange which favours an AF spin arrangement and 'double' exchange which promotes ferromagnetic spin order. Though there has been a great deal of effort made to understand the magnetic structure on the basis of spin–spin interaction in the presence of Jahn–Teller lattice distortion and 'double' exchange, there has been little attempt to understand the nature of the charge carrier and its transport properties, which is essential for exploring the origin of the CMR effect. Palstra *et al* [12] have recently reported on the transport properties of doped $LaMnO_3$. They find that above the magnetic transition temperature the charge carriers behave as polarons and the transport is not dominated by the spin disorder. Furthermore, Bahadur *et al* [13] find that some CMR systems exhibiting identical magneto-transport properties possess very different magnetic properties. This suggests that the behaviours of both the localized and the mobile charge carriers are strongly influenced by

0953-8984/99/234539+17$19.50

the long-range orbital and spin order. The transport properties should therefore be examined with the presence of coupling of the mobile charge carriers to lattice vibrations and magnetic order.

In this paper we start with the effective Hamiltonian of Ishihara *et al* [5] which describes the spin and orbital coupling between neighbouring Mn^{3+} ions in $LaMnO_3$. The magnetic coupling is then expressed in a form close to the Heisenberg model for a layered spin structure. On doping, the delocalized e_g electron is described by the Holstein Hamiltonian for a small polaron [14] and its transport properties are analysed with bond and spin order present in the lattice. An expression for the electrical conductivity by polaron hopping is obtained using the method followed by Reik [15]. For compounds which have ions with mixed-valence states at crystallographically equivalent sites, the configurational and magnetic energies remain unchanged if the ions of one kind simultaneously exchange their sites with ions of the other kind. This case of correlated polaron motion has been considered by us for ferrites [16] and for oxide superconductors [17] and has been applied in the present case to manganites. It has been shown that the activation energy for dc electrical conductivity obtained on the basis of correlated polaron transport contains a term that depends on the product of the magnetic and bond order parameters. The activation energy therefore varies rapidly near the magnetic transition temperature, which accounts for the existence of the colossal magnetoresistance observed in this system.

2. The effective Hamiltonian for localized and delocalized electrons

It has been shown by Ishihara *et al* [5] that the effective Hamiltonian for an electron in a doubly degenerate e_g orbital coupled to t_{2g} spins in Mn^{3+} can be written as

$$H_{\rm eff} = H_{e_g} + H_{t_{2g}} \tag{1}$$

$$H_{e_g} = \sum_{i,\tau,\sigma} \varepsilon_d c^{\dagger}_{i\tau\sigma} c_{i\tau\sigma} + \sum_{\substack{ij\sigma \\ \tau\tau'}} (t^{\tau\tau'}_{ij} c^{\dagger}_{i\tau\sigma} c_{i\tau'\sigma} + \mathrm{HC}) + U \sum_{i\tau} n_{i\tau_\uparrow} n_{i\tau_\downarrow} + U' \sum_{i\sigma} n_{i\alpha\sigma} n_{i\beta\sigma}$$
$$- J' \sum_i \boldsymbol{\sigma}_{i\alpha} \cdot \boldsymbol{\sigma}_{i\beta} - K(\boldsymbol{\sigma}_{i\alpha} + \boldsymbol{\sigma}_{i\beta}) \cdot \boldsymbol{S}_i \tag{2}$$

$$H_{t_{2g}} = J^{t_{2g}} \sum_{ij} \boldsymbol{S}_i \cdot \boldsymbol{S}_j. \tag{3}$$

In equation (2), $c^{+}_{i\tau\sigma}$ ($c_{i\tau\sigma}$) represents the creation (destruction) operator for the doubly degenerate e_g electron in the τ-orbital ($\tau = \alpha, \beta$) with spin $\boldsymbol{\sigma}$ and $\boldsymbol{S}$ is the spin of the t_{2g} electron. The first term describes the level energy, ε_d, of the e_g electron, $t^{\tau\tau'}_{ij}$ denotes the electron transfer integral for transfer from site i and orbit τ to orbit τ' on a near-neighbour site j, U and U' are intra- and inter-orbital Coulomb integrals, J' denotes the inter-orbital exchange and K describes the Hund coupling. Equation (3) describes the near-neighbour AF interaction amongst the t_{2g} electrons. Since the electron–electron interaction in equation (2) has the largest energy scale, H_{e_g} excludes double occupancy of the e_g orbitals. The second-order perturbation processes involving the inter-site hopping integral $t^{\tau\tau'}_{ij}$ lead to anisotropic ferromagnetic interaction when an electron hops from an occupied orbital τ ($=\alpha$) at i to an unoccupied orbital τ' ($=\beta$) at j. It has been shown [5] that in the presence of $(3x^2 - r^2/3y^2 - r^2)$-type ordering in $LaMnO_3$ the electron transfer to unoccupied $(y^2 - z^2/z^2 - x^2)$ orbitals at nn sites results in a ferromagnetic coupling between ionic spins in the ab-plane much larger than what is produced in the c-direction by the isotropic AF $J^{t_{2g}}$ interaction and accounts for the A-AF structure observed in this compound. We express this anisotropic spin–spin coupling in the form of a Heisenberg

Hamiltonian. An expression for the contribution to the effective Hamiltonian from the second-order perturbation process with respect to the electron transfer, $H_{\rm eff}^{\rm SO}$, can be given [5] in terms of the pseudo-spin operator, $\boldsymbol{\tau}$, in the orbital space with $\tau_z = 1/2$ and $-1/2$ denoting the states in which $\alpha = 3x^2 - r^2$ and $\beta = z^2 - y^2$, respectively, are occupied and the total spin $\boldsymbol{I} = \boldsymbol{\sigma} + \boldsymbol{S}$ where $\boldsymbol{\sigma}$ is the spin of the e_g electron and $\boldsymbol{S}$ is the spin of the t_{2g} electron. The coupling between spins is such that $\boldsymbol{\sigma} = (1/4)\boldsymbol{I}$ and $\boldsymbol{S} = (3/4)\boldsymbol{I}$. For $t^{\alpha\alpha} = t^{\beta\beta} = 0$,

$$H_{\rm eff}^{\rm SO} = -\frac{2}{U' - J}\sum_{ij}\frac{1}{16}(4n_i n_j + I_i I_j)\left[(t_{ij}^{\alpha\beta 2} + t_{ij}^{\beta\alpha 2})\left(\frac{1}{4}n_i n_j + \tau_{iz}\tau_{jz}\right)\right.$$
$$\left. - t_{ij}^{\alpha\beta}t_{ij}^{\beta\alpha}(\tau_{i+}\tau_{j+} + \tau_{i-}\tau_{j-})\right] + \frac{9}{16}J'^{t_{2g}}\sum_{ij}\boldsymbol{I}_i \cdot \boldsymbol{I}_j \tag{4}$$

where n_i is the number operator at site i. Equation (4) shows that there is strong coupling between the spin and orbital degrees of freedom. The spin–spin coupling can be written in the following form, comprising an isotropic term, J, and an anisotropic term containing a symmetric tensor, Γ_{ij}:

$$H_{\rm s} = -2J\sum_{ij}\boldsymbol{I}_i \cdot \boldsymbol{I}_j - 2\sum_{ij}\boldsymbol{I}_i \cdot \Gamma_{ij} \cdot \boldsymbol{I}_j \tag{5}$$

where

$$J = -(9/32)J^{t_{2g}} \tag{6}$$

and

$$\Gamma_{ij} = \frac{1}{16(U' - J')}\left[\left(t_{ij}^{\alpha\beta 2} + t_{ij}^{\beta\alpha 2}\right)\left(\frac{1}{4}n_i n_j + \tau_{iz}\tau_{jz}\right) - t_{ij}^{\alpha\beta}t_{ij}^{\beta\alpha}(\tau_{i+}\tau_{j+} + \tau_{i-}\tau_{j-})\right]. \tag{7}$$

We express the exchange integral as [18]

$$J_{ij} = -\frac{1}{4S_i S_j}\left(\sum_k \frac{2b_k^2}{U_k}\right) \tag{8}$$

where b_k is a one-electron matrix element that connects the two ions and U_k is the on-site repulsion energy. The summation over k extends over all possible routes of the super-exchange interaction. If b_σ and b_π denote the effective electron transfer integrals along the σ- and π-bond directions, respectively, then

$$J = -\frac{1}{16}\left[\frac{4b_\pi^2}{U' - J'}\right] \tag{9}$$

and

$$\Gamma_{aa} = \frac{1}{N}\sum_{ij}\Gamma_{ij} = \frac{1}{16}\left[\frac{2b_\sigma^2}{U' - J'}\right] \qquad \Gamma_{bb} = 0 \qquad \Gamma_{cc} = 0. \tag{10}$$

Here a denotes the e_g-bond direction in the ab-plane and N denotes the number of Mn ions. An estimate of J and Γ_{aa} can be made from the spin-wave spectrum. For $LaMnO_3$ the width of the spin-wave spectrum is determined using neutron scattering and is approximately 32 and 5 meV along the ab-plane and the c-direction respectively [19]. This gives $J = 0.62$ meV. To fit the dispersion curve of the spin wave, a value of 6.5 meV is taken for $J^{t_{2g}}$ in reference [5] which is three times larger than the value obtained by us. The width of the spin-wave spectrum along $(\pi/a, \pi/a, 0)$ is 32 meV. Taking $J_{\rm eff} = [\Gamma_{aa}J]^{1/2}$, we get $\Gamma_{aa} = 1.61$ meV. From equations (9) and (10) the values of b_σ and b_π, with $U' = 5$ eV and $J' = 2$ eV as used in reference [5], are 0.20 and 0.09 eV respectively. For spinel ferrites the values of the transfer

integrals for 180° super-exchange interaction with $U = 10$ eV, $J = 0$ are $b_\sigma = 0.31$ eV and $b_\pi = 0.18$ eV [20]. These values are comparable for manganites and ferrites despite the fact that the energies of the intermediate states in the two cases are different by almost a factor of three.

The exclusion of doubly occupied e_g states in $LaMnO_3$ prevents first-order perturbation processes involving electron transfer. On doping, mobile charge carriers are introduced which initiate the 'double-exchange' process. We examine it in terms of small-polaron formation and transfer in the presence of orbital and spin order. Following Holstein [14], we express the Hamiltonian for the electron using the first two terms in equation (2) and add the Hamiltonian for the phonon and the electron–phonon interaction:

$$H^{\mathrm{p}}_{\mathrm{eff}} = H_{\mathrm{e}} + H_{\mathrm{ph}} + H_{\mathrm{ep}} \tag{11}$$

$$H_{\mathrm{e}} = \sum_{i\sigma} \varepsilon_{\mathrm{d}} c^{\dagger}_{i\sigma} c_{i\sigma} + \sum_{\substack{ij \\ \sigma\sigma'}} \left(t^{\mathrm{p}}_{ij\ \sigma\sigma'} c^{\dagger}_{i\sigma} c_{j\sigma'} + \mathrm{HC} \right) \tag{12}$$

$$H_{\mathrm{ph}} = \sum_{q\lambda} \hbar\omega_{q\lambda} a^{\dagger}_{q\lambda} a_{q\lambda} \tag{13}$$

$$H_{\mathrm{ep}} = \sum_{q\lambda i} \hbar\omega_{q\lambda} \alpha^{1/2}_{\lambda}(q)\mathrm{i}(a_{q\lambda}\mathrm{e}^{\mathrm{i}qR_i} - a^{\dagger}_{q\lambda}\mathrm{e}^{-\mathrm{i}qR_i)}) c^{\dagger}_i c_i. \tag{14}$$

The electron transfer $t^{\mathrm{p}}_{ij\ \sigma\sigma'}$ occurs due to the electron–phonon coupling in equation (14). $\alpha_\lambda(q)$ denotes the electron–phonon coupling constant and is defined in terms of the optical deformation potential constant. Reik [15], starting with $H^{\mathrm{p}}_{\mathrm{eff}}$, uses the polaron canonical transformation to obtain the following Hamiltonian for the polaron and displaced phonons:

$$H^{\mathrm{p}'}_{\mathrm{eff}} = H_{\mathrm{pol}} + H'_{\mathrm{ph}} \tag{15}$$

$$H_{\mathrm{pol}} = \sum_i (\varepsilon_{\mathrm{d}} - \varepsilon_{\mathrm{p}}) l^{\dagger}_i l_i + \sum_{ij} (t^{\mathrm{p}}_{ij} l^{\dagger}_i l_j X_{ij} + \mathrm{HC}) \tag{16}$$

$$H' = \sum_{q\lambda} \hbar\omega_{q\lambda} b^{\dagger}_{q\lambda} b_{q\lambda} \tag{17}$$

where $\sigma = \sigma'$. Here $l^{\dagger}_i$ (l_i) denotes the creation (destruction) of a polaron at site i, $b^{\dagger}_{q\lambda}$ ($b_{q\lambda}$) denotes the creation (destruction) of a displaced phonon of wave vector q and polarization λ and X_{ij} denotes the Frank–Condon (FC) transitions. The ground-state energy in equation (16) is lowered by an amount ε_{p} by the electron–phonon interaction.

It follows from equation (5) that localized e_g electrons in Mn interact through H_{s} which, along with bond order, leads to an A-AF spin structure in $LaMnO_3$. On doping, the mobile electrons are introduced into the system. As discussed by de Gennes [11], the effect of hopping charge carriers in the antiferromagnetic lattice is to distort the ground-state spin arrangement, since hopping reduces the energy by a term of first order in the distortion angle while the loss of A-AF exchange energy is of second order. Starting with an A-AF spin arrangement in which spins are coupled ferromagnetically to the spins in the same layer and antiferromagnetically to the spins in the adjacent layers, as in figure 1(a), de Gennes shows that in the presence of double exchange the magnetization of successive layers makes an angle θ, which is given by

$$\cos\frac{\theta}{2} = \frac{\varepsilon_{\mathrm{p}} x}{4JS^2} \tag{18}$$

where x is the concentration of the charge carriers, ϵ_{p} is the gain in the energy due to hopping and the A-AF coupling between the spins in the adjacent layers is caused by the t_{2g} spins. Using the neutron diffraction data of Wollan and Koehler [7], de Gennes [11] has estimated a

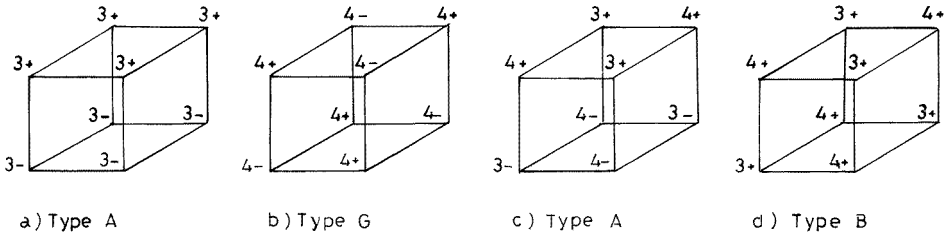

Figure 1. The spin arrangement on an octant of a magnetic unit cell in (a) $LaMnO_3$ (type A), (b) $CaMnO_3$ (type G), (c) $Nd_{0.5}Sr_{0.5}MnO_3$, antiferromagnet, insulating, $0 \leqslant T < 160$ K (type A), (d) $Nd_{0.5}Sr_{0.5}MnO_3$, ferromagnetic, conducting, $160 < T \leqslant 265$ K (type B).

value of 16 for ϵ_p/JS^2 for $La_{1-x}Ca_xMnO_3$. Taking $J = 0.62$ meV, $S = 3/2$ gives $\epsilon_p = 268$ K. We show later that for manganites the resistivity data give a value for ϵ_p ranging between 70 K and 600 K.

The spin arrangement for $\epsilon_p = 250$ K obtained using equation (18) is that of a collinear ferromagnet for $x > 0.26$. Following de Gennes, the Curie temperature for a ferromagnetic spin arrangement in $La_{1-x}Ca_xMnO_3$ is given by

$$k_B T_c = \frac{2}{3}\left[z_a|J^a| - z_b|J^b| - z_c|J^c|\right] I^2 + \frac{2xz\varepsilon_p}{5} \tag{19}$$

while for the insulating A-AF spin arrangement the Néel point is given by

$$k_B T_N = \frac{2}{3}\left[z_a|J^a| - z_b|J^b| + z_c|J^c|\right] I^2 \tag{20}$$

where the z_i ($i = a, b, c$) are the numbers of nearest neighbours along the a-, b-, c-directions, z is the total number of nearest neighbours and J^i is the effective J in the i-direction. Taking $J^a = 1.61$ meV, $J^b = J^c = 0.62$ meV, $x = 0.33$ meV, $\epsilon_p = 250$ K, we obtain $T_c = 222$ K for $La_{0.67}Ca_{0.33}MnO_3$, close to the experimental value of 235 K [21]. This calculation of T_c is made assuming that there is no change in the value of J^i and ε_p as x is increased from 0 to 0.33. However, as the number of Jahn–Teller ions varies with x, the lattice distortion produced by the JT effect changes both the crystal and magnetic energies. Taking 90 K for T_N for $CaMnO_3$ with $J^a = J^b = J^c$, we get a value of 0.55 meV for J which is smaller than that of 0.62 meV observed for $LaMnO_3$. The spin arrangement due to isotropic t_{2g} AF interaction is a G-type AF one, shown in figure 1(b).

Recently, a transition from an AF insulating to a ferromagnetic metallic state at 160 K has been reported for $Nd_{0.5}Sr_{0.5}MnO_3$ by Caignaert *et al* [22]. They attributed the metallic properties to the absence of JT distortion of Mn ions in the orthorhombic phase obtained at RT. We can take the magnetic order in the insulating phase as A-AF, shown in figure 1(c). In that case, equation (20) applies. Taking $J^b = J^c = 0.62$ meV, we obtain $J^a = 2.5$ meV. In the ferromagnetic phase the spin arrangement is that of a B-type ferromagnet shown in figure 1(d). In this case, a ferromagnetic contribution from mobile charge carriers enters, as in equation (19). From $T_c = 265$ K we obtain $\varepsilon_p = 204$ K, in reasonable agreement with the observed values for manganites. The resistivity data clearly show the thermodynamic transition from an AF to a ferromagnetic phase and indicate an interesting dependence of the resistivity on the magnetic structure. The resistivity varies as $m^2(t)$ where $m(t)$ is the reduced sublattice magnetization of the antiferromagnetic lattice at the reduced temperature $t = T/T_N$. In the ferromagnetic phase it is also a function of $m(t)$. We discuss the relationship between the electrical resistivity and the atomic and magnetic order in section 4.

3. Electrical conductivity

The Hamiltonian in equation (16) has been used by Reik [15] to obtain expressions for the dc and optical conductivity following Kubo's current–current correlation formulation. Recently we have used it [23] to explain the dc conductivity and photoemission and femtosecond spectroscopy results for oxide superconductors. It has been shown that the dc conductivity by polaron hopping for a simple cubic structure is given by

$$\sigma_{\rm hop} = \frac{\sqrt{\pi}}{2} n \left(\frac{t^{\rm p}}{\overline{h}}\right)^2 e^2 a^2 \beta \tau \, {\rm sech}^2\left(\frac{\varepsilon_{\rm p}\beta}{2}\right) {\rm e}^{-U_{\rm H}\beta}. \tag{21}$$

Here n represents the number of polarons, $\beta = 1/k_{\rm B}T$, a is the separation of the nearest neighbours between which the electron hops, τ is the relaxation time and $U_{\rm H}$ represents the activation energy of the dc mobility. For mixed-valence compounds where correlated polaron transport occurs without FC transitions we obtain a similar expression for the hopping conductivity [17] but with the conditions

$$U_{\rm H} = 0 \tag{22a}$$

$$\tau^{-1} = \frac{t^{\rm p}}{\overline{h}} = \omega_{\rm ph}. \tag{22b}$$

A classical method for estimating $\varepsilon_{\rm p}$ based on the Madelung energy for a linear chain has been given by us [16]. We note from equation (21) that the correlated polaron hopping mobility satisfies the Einstein relation for diffusivity:

$$\mu_{\rm p} = e\left(\frac{\omega_{\rm ph}}{2\pi}\right) a^2 \beta \exp(-U_{\rm H}\beta) \tag{23a}$$

and the concentration of the charge carriers varies with T as

$$n(T) = n \, {\rm sech}^2(\varepsilon_{\rm p}\beta/2). \tag{23b}$$

The bond and spin orders for uncorrelated polarons when FC transitions occur affect the relaxation time τ and the dc activation energy $U_{\rm H}$ in equation (21). It was shown by Reik that τ and $U_{\rm H}$ both depend on the average number of phonons $n_{\rm ph}$ in the cloud of the polaron. For $T > \theta_{\rm D}/4$,

$$\frac{1}{\tau} = \left(\frac{2n_{\rm ph}}{\sinh(\overline{h}\omega_0\beta/2)}\right)^{1/2} \omega_0 \tag{24}$$

$$U_{\rm H} = \sum_{q\lambda} \alpha_\lambda(q) \sin^2\left(\frac{1}{2}\boldsymbol{q}\cdot\boldsymbol{a}\right) \overline{h}\omega_\lambda(q) \simeq \frac{1}{4} n_{\rm ph} \overline{h}\omega_0 \tag{25}$$

where ω_0 is an average longitudinal optical phonon frequency. Mott and collaborators [24] obtained an expression for the dc conductivity similar to equation (21) except that the transfer integral $t^{\rm p}$ contains an electron overlap term, $\exp(-2\gamma a)$, such that

$$\left(\frac{t^{\rm p}}{\overline{h}}\right)^2 \tau \simeq \omega_0 \exp(-2\gamma a) \tag{26}$$

and

$$\sigma_{\rm hop}^{\rm M} = An\omega_0 e^2 a^2 \beta \exp(-2\gamma a) \exp(-U\beta) \tag{27}$$

where U comprises two terms, one ($U_{\rm D}$) arising from atomic disorder and the other ($U_{\rm H}$) arising from thermally activated hopping as indicted in equation (21):

$$U = \begin{cases} U_{\rm H} + U_{\rm D} & \text{for } T > \theta_{\rm D}/2 \quad (28a) \\ U_{\rm D} & \text{for } T < \theta_{\rm D}/2. \quad (28b) \end{cases}$$

We have recently found evidence of polaronic transport with and without FC transitions in oxide superconductors [23] and consider that this occurs in manganites also. To determine τ and $U_{\rm H}$ we therefore discuss the atomic and magnetic long- and short-range orders in manganites. According to the estimates of Ishihara *et al* [5], the orbital ordering temperature for $LaMnO_3$ is much higher than the spin ordering temperature. The method for determining the bond ordering temperature is discussed below.

4. Long- and short-range order

We consider a ferromagnetic binary alloy AB and, following Muto *et al* [25], examine the dependence of the order on temperature using the Ising model in which the spins are parallel and anti-parallel. We consider the internal energy associated with the bond energies of AA, AB and BB nn pairs and denote them as ν_{ij} $(i, j = {\rm A}, {\rm B})$. Since separating bond and charge orders is difficult, we use a simplified approach. For $LaMnO_3$ we take A and B as the α- and β-states of the e_g electron, while for $La_{0.5}Ca_{0.5}MnO_3$ in the metallic state we treat Mn^{3+} and Mn^{4+} ions as A and B. For intermediate values of x we take bond or charge (atomic) order depending upon the situation. We denote the total numbers of nearest neighbours as follows:

$$\begin{aligned}
&\sum_{\substack{ij\\ \sigma\sigma'}} A_i(\sigma)A_j(\sigma') = Q_{\rm AA} = Q_{\rm AA}(\uparrow\uparrow) + Q_{\rm AA}(\uparrow\downarrow)\\
&\sum_{\substack{ij\\ \sigma\sigma'}} B_i(\sigma)B_j(\sigma') = Q_{\rm BB} = Q_{\rm BB}(\uparrow\uparrow) + Q_{\rm BB}(\uparrow\downarrow)\\
&\sum_{\substack{ij\\ \sigma\sigma'}} A_i(\sigma)B_j(\sigma') = Q_{\rm AB} = Q_{\rm AB}(\uparrow\uparrow) + Q_{\rm AB}(\uparrow\downarrow).
\end{aligned} \tag{29}$$

The energies ν_{ij} $(i, j = {\rm A}, {\rm B})$ depend on the spins σ, σ' and states α, β of the occupied e_g orbital as can be seen in equations (4) and (16). The bond order–disorder temperature of $LaMnO_3$ can therefore be expressed as

$$k_{\rm B}T_{\rm ca} = E'_{\rm b} \tag{30}$$

where

$$E'_{\rm b} = \frac{4\nu(Q^{\alpha\alpha}_{\rm AA}(\uparrow\uparrow) + Q^{\beta\beta}_{\rm AA}(\uparrow\uparrow) + 2Q^{\alpha\beta}_{\rm AA}(\uparrow\uparrow))}{Q} \tag{31}$$

$$\nu = \nu^{\alpha\beta}_{\rm AA}(\uparrow\uparrow) - \left(\frac{\nu^{\alpha\alpha}_{\rm AA}(\uparrow\uparrow) + \nu^{\beta\beta}_{\rm AA}(\uparrow\uparrow)}{2}\right) \tag{32}$$

$$Q = \frac{Nz}{2} \tag{33}$$

for $\sigma = \sigma'$. Here N is the total number of Mn atoms, z is the number of nearest neighbours and Q is the total number of nearest-neighbour pairs. For doped manganites, the polaron stabilization energy $\epsilon_{\rm p}$ depends on the Mn^{3+}–Mn^{4+} pairs. If this dominates, ν is given by

$$\nu = \sum_{i=\alpha,\beta}\left[\nu^{ii}_{\rm AB}(\uparrow\uparrow) - \left(\frac{\nu^{ii}_{\rm AA}(\uparrow\uparrow) + \nu^{ii}_{\rm BB}(\uparrow\uparrow)}{2}\right)\right]. \tag{34}$$

Following Muto *et al* [25], we define the bond (atomic) long-range ($S_{\rm a}$) and bond (atomic) short-range ($\sigma_{\rm a}$) order parameters as follows:

$$S_{\rm a} = \frac{(r^{\uparrow} + r^{\downarrow}) - (r^{\uparrow} + r^{\downarrow})_{\rm r}}{(r^{\uparrow} + r^{\downarrow})_{\rm m} - (r^{\uparrow} + r^{\downarrow})_{\rm r}} \tag{35}$$

$$\sigma_{\mathrm{a}} = \frac{q - q_{\mathrm{r}}}{q_{\mathrm{m}} - q_{\mathrm{r}}} \tag{36}$$

$$q = \frac{Q_{\mathrm{AB}}}{Q}. \tag{37}$$

Here the subscripts m and r stand for maximum and random and refer to values at $T = 0$ and $T > T_{\mathrm{c}}$. $r^{\uparrow}$ denotes the right bond (atom) with spin up. The magnetic long-range order, S_{m}, is defined as

$$S_{\mathrm{m}} = \frac{(r^{\uparrow} + w^{\downarrow}) - (r^{\uparrow} + w^{\downarrow})_{\mathrm{r}}}{(r^{\uparrow} + w^{\downarrow})_{\mathrm{m}} - (r^{\uparrow} + w^{\downarrow})_{\mathrm{r}}} \tag{38}$$

where $w^{\uparrow}$ denotes the wrong bond (atom) with spin up. The activation energy U_{H} in equation (25) depends on the phonon wave vector $\boldsymbol{q}$ and the charge-carrier transfer vector, $\boldsymbol{X}_i - \boldsymbol{X}_j = \boldsymbol{a}$ where $\boldsymbol{X}_i$ and $\boldsymbol{X}_j$ denote the position vectors before and after the jump. We have further seen that the probabilities of virtual and real transfers depend on the bond and spin order as well as on the charge order when itinerant states are introduced on doping. On the basis of equations (21), (25) and (28), we express the activation energy of manganites as

$$U = U_0 \xi^2 \tag{39}$$

$$U_0 = \frac{1}{2}\langle\alpha\rangle\langle\hbar\omega\rangle = \frac{1}{4} n_{\mathrm{ph}} \hbar\omega_0 \tag{40}$$

$$\xi^2 = \begin{cases} \langle \sin^2(\frac{1}{2}\boldsymbol{q}\cdot\boldsymbol{a})\rangle = S_{\mathrm{a}}^2(1 - S_{\mathrm{m}})^2\sigma_{\mathrm{a}}^2 & \text{for } T < T_{\mathrm{ca}} \\ \sigma_{\mathrm{a}}^2 & \text{for } T > T_{\mathrm{ca}} \end{cases} \tag{41}$$

where S_{a}, σ_{a} and S_{m} are defined above. For $\boldsymbol{q}$ normal to $\boldsymbol{a}$, $\xi = 0$. This, along with equation (22*b*), describes the motion of the correlated polaron in which the activation energy vanishes and the transfer integral and relaxation time are determined by the longitudinal optical phonon frequencies. In the presence of magnetic interactions between the mobile and localized charge carriers in manganites, in addition to the contribution from phonons to τ in equation (24), there occurs a contribution, τ_{s}, from spin–spin scattering. Following Fisher and Langer [26] it can be shown that for ferromagnetic spin arrangement

$$\frac{1}{\tau_{\mathrm{s}}} = \frac{1}{\tau}(1 - m^2(t))\sigma_{\mathrm{a}}^2 \tag{42}$$

where $m(t)$ is the reduced magnetization at the reduced temperature $t = T/T_{\mathrm{c}}$. We get finally

$$\frac{1}{\tau_{\mathrm{eff}}} = \frac{1}{\tau} + \frac{1}{\tau_{\mathrm{s}}}. \tag{43}$$

If the magnetic order S_{m} in equation (41) is not equal to 1, $U = U_{\mathrm{H}}$ does not vanish in equation (21). The dc hopping resistivity in the correlated small-polaron model is then given by

$$\rho_{\mathrm{hop}}^{\mathrm{c}} = \frac{AT}{n}\left[1 + \left\{1 - m^2(t)\right\}\sigma_{\mathrm{a}}^2\right]\cosh^2\left(\frac{\varepsilon_{\mathrm{p}}}{2T}\right)\exp(U/T) \tag{44}$$

where

$$A = \frac{1.13 k_{\mathrm{B}}}{\omega_{\mathrm{ph}} a^2 e^2}. \tag{44a}$$

Here ϵ_{p} and U are expressed in temperature units. For an antiferromagnetic lattice, as spin–spin scattering dominates over that due to phonons given in equation (24), and hopping occurs only for parallel spins,

$$\frac{1}{\tau_{\mathrm{eff}}} = \frac{1}{\tau_0} m_{\mathrm{A}}^2(t) \tag{45}$$

where $m_A(t)$ is the reduced magnetization of one of the two sublattices that are coupled antiferromagnetically at the reduced temperature $t = T/T_N$ and τ_0 is a relaxation time independent of T. In that case, in the AF region the resistivity of the correlated polaron is

$$\rho_A^c = \rho_{0A} m_A^2(t) \cosh^2\left(\frac{\varepsilon_p}{2T}\right) \tag{46}$$

while in the ferromagnetic region it is given by

$$\rho_F^c = \rho_{0F}[1 + \{1 - m_F^2(t)\}\sigma_a^2] \cosh^2\left(\frac{\varepsilon_p}{2t}\right). \tag{47}$$

Here ρ_{0A} and ρ_{0F} are constants independent of T and $m_F^2(t)$ is the reduced magnetization in the ferromagnetic region. The temperature dependence of the resistivity for $Nd_{0.5}Sr_{0.5}MnO_3$ given by Caignaert *et al* in reference [22] fits equation (46) over the range $10 < T < 160$ K and equation (47) over the range $160\ \text{K} < T \leqslant 265$ K for the following parameters: $\rho_{0A} = 0.4\ \Omega$ cm, $\rho_{0F} = 1.4 \times 10^{-3}\ \Omega$ cm, $m_A(t) = m_F(t) = (1 - t^2)^{1/2}$, $\sigma_a = 1$, $\varepsilon_p = 30$ K, $T_N = 160$ K and $T_c = 265$ K. Equation (46) explains the unusual upturn in the resistivity curve for $T < 40$ K and equation (47) accounts for the temperature independence of the resistivity for $T > T_c$. This supports a polaronic nature for the charge carriers.

We take the following analytical forms for S_a and σ_a which approximately fit the values of these parameters for AB_3 alloys obtained by Nix and Shockley [27]:

$$S_a = (1 - 0.6t_{ca}^3)^{1/2} \qquad \text{for } t_{ca} < 1 \tag{48a}$$

$$\sigma_a = (1 - 0.75t_{ca}^3)^{1/2} \qquad \text{for } t_{ca} \leqslant 1 \tag{48b}$$

$$S_a = 0 \qquad \text{for } t_{ca} > 1 \tag{48c}$$

$$\sigma_a = (1 - 0.9t_{ca}^{0.25})^{1/2} \qquad \text{for } t_{ca} > 1 \tag{48d}$$

$$S_m = m(t) = (1 - t^2)^{1/2} \qquad \text{for } t < 1 \tag{48e}$$

$$t_{ca} = T/T_{ca} \qquad t = T/T_c. \tag{48f}$$

The analysis of the resistivity data yields both T_c and T_{ca}. We show later, in section 6, that equation (44) leads to an expression for the magnetoresistance which is in agreement with experiment.

5. The temperature dependence of the magnetization

We have seen that the resistivity is dependent on the magnetization, so the temperature and field dependence of the magnetization is required to study the magnetoresistance in doped perovskite manganites. Most of the interesting CMR studies reported are for $0.26 \leqslant x \leqslant 0.5$ in which the spin arrangement is usually that of a collinear ferromagnet. We restrict our discussion to this region. Since the total spin $\boldsymbol{I}$ is such that $\boldsymbol{\sigma} = \frac{1}{4}\boldsymbol{I}$ and $\boldsymbol{S} = \frac{3}{4}\boldsymbol{I}$, we treat the system within the Ising model of the ferromagnetic binary alloy. The spins are collinear and constitute four groups, $A_1(Mn^{3+}\uparrow)$, $A_2(Mn^{4+}\uparrow)$, $B_1(Mn^{3+}\downarrow)$ and $B_2(Mn^{4+}\downarrow)$. A magnetic Bravais lattice exists for $A_{1-x}B_xMn^{3+}_{1-x}Mn^{4+}_xO_3$ for $x = n/8$ where n is an integer, and has a cell constant $2a$, which is double that of the chemical cell. The moments occupy eight corners and twelve edge-centre, one body-centre and six face-centre positions of the cube and there are eight Mn atoms per unit magnetic cell.

We have seen in section 2 that the Mn^{3+}–Mn^{3+} interaction in $LaMnO_3$ is highly anisotropic, with $J^a = 1.61$ meV $= +19$ K and $J^c = -0.62$ meV $= -7.5$ K. On doping, when mobile charge carriers are introduced, an isotropic ferromagnetic interaction is introduced through double exchange which, according to de Gennes [11], cannot be expressed in pairwise $\boldsymbol{I}_i \cdot \boldsymbol{I}_j$

form. The dependence of the magnetization on temperature is calculated using the Weiss-field approximation. In the Ising model with moments distributed on four sublattices, we need to specify three exchange constants which describe the energy of interaction of Mn^{3+}–Mn^{3+}, Mn^{4+}–Mn^{4+} and Mn^{3+}–Mn^{4+} ion pairs. Of these, we obtained an estimate of the antiferromagnetic $J(Mn^{4+}–Mn^{4+})$ for $La_{1-x}Ca_xMnO_3$. It is -0.62 meV for $x = 0$ and -0.55 meV for $x = 1$. As T_c for $A_{1-x}B_xMnO_3$ depends on the A and B cations and varies from 80 K to 400 K, we assume that the dominant interaction $J(Mn^{3+}–Mn^{4+})$ in the collinear ferromagnet spin arrangement changes from 5 K to 20 K. For T_c nearly 150 K, we take the following exchange constants:

$$\begin{aligned} J_1 &= J(Mn^{3+}–Mn^{3+}) = -7.9\ \text{K} \\ J_2 &= J(Mn^{4+}–Mn^{4+}) = -6.7\ \text{K} \\ J_3 &= J(Mn^{4+}–Mn^{3+}) = 6.0\ \text{K}. \end{aligned} \tag{49}$$

The Js in equation (49) require that if ions in groups A_1 and B_2 occupy the sites (000) and (aa0), then those in A_2 and B_1 occupy (a00) and (aaa). The ions in groups A_1 and A_2 constitute a magnetic sublattice P and those on B_1 and B_2 constitute a sublattice Q. It is convenient to express the magnetization in terms of four sublattices A_1, A_2, B_1 and B_2 formed by the ions in the four groups. The magnetic moment per Mn atom, $\boldsymbol{\mu}$, assuming collinear spin arrangement and spin-only values is

$$\bar{\mu} = \frac{1}{N}\left[4\{n(A_1) - n(B_1)\} + 3\{n(A_2) - n(B_2)\}\right] \tag{50}$$

where $n(q_i)$ ($q = A, B$, $i = 1, 2$) denotes the number of Mn atoms in the sublattice q_i and N is the total number of Mn atoms. The magnetization of the q_i-sublattice in the molecular-field approximation is

$$M_{q_i}(T) = M_{q_i}(0)B_{s_{q_i}}(x_{q_i}) \qquad (q_i = A_1, A_2, B_1, B_2) \tag{51}$$

where

$$x_{q_i} = \left(\frac{s_{q_i} g_{q_i} \mu_B}{k_B T}\right) H_{q_i} \tag{52}$$

$$M_{q_i}(0) = \left(\frac{n_{q_i} s_{q_i} g_{q_i} \mu_B}{8a^3}\right) \tag{53}$$

with the Weiss field given by

$$H_{q_i} = \sum_{q_j} \lambda_{q_i q_j} M_{q_j} \tag{54}$$

$$\lambda_{q_i q_j} = \frac{2 z_{q_i q_j} J_{q_i q_j}}{N_{q_j} g_{q_i} g_{q_j} \mu_B^2} \tag{55}$$

where $z_{q_i q_j}$ is the number of nearest neighbours on the jth sublattice to an atom on the ith sublattice. N_j is the number of atoms per unit volume on the jth sublattice, g_i and g_j are the Landé factors for the ions on the ith and jth sublattices respectively and μ_B is the Bohr magneton. The magnetization is obtained from equation (51). The effect of double exchange which contributes nearly $+bx/4S^2$ to the exchange constant can be take into account by suitably modifying the value of J_3 to fit the experimental results. It is easily verified that in the present case out of sixteen only four Weiss-molecular-field constants are nonvanishing. These are $\lambda_{A_1A_2}$, $\lambda_{A_1B_1}$, $\lambda_{A_2B_2}$ and $\lambda_{B_1B_2}$. A computer program is used to obtain the temperature dependence of the magnetization using equations (51) and (54) and this is shown in figure 2 for $La_{1-x}Ca_xMnO_3$ with $x = 0.375, 0.5$. The values of $M_s(0)$ and T_c are given in table 1. The

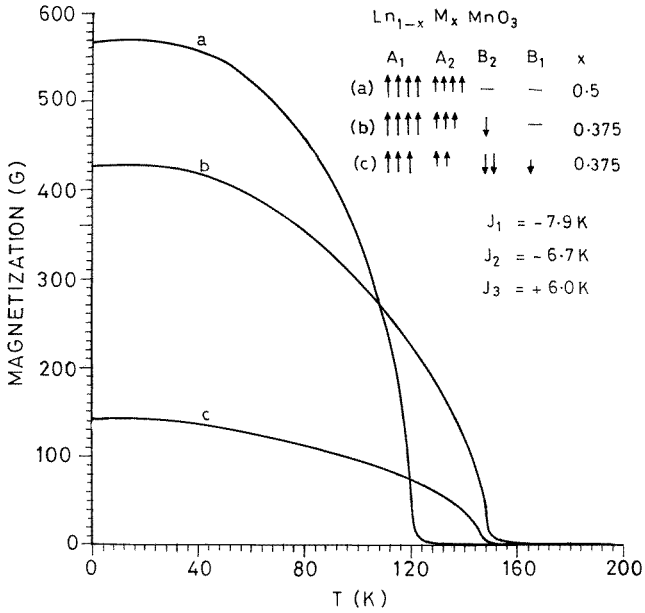

Figure 2. Computer solutions for the magnetization curves obtained using equations (51) and (53) (see the text) for the sublattice arrangements shown in table 1. For curve (a), $A_{\bar{1}}$ and $A_{\bar{2}}$ sublattices are occupied; for curve (b), $A_{\bar{1}}$, $A_{\bar{2}}$, $B_{\bar{2}}$ are occupied; for curve (c), all four sublattices are occupied. The values of the exchange constants are taken as $J_1 = -7.9$ K, $J_2 = -6.7$ K and $J_3 = +6.0$ K.

Table 1. Values of $\bar{\mu}$, $M_s(0)$ and T_c obtained for the magnetic order on the 4-sublattices of $La_{1-x}Ca_xMnO_3$ for $x = 0.5$ and 0.375, with ordering denoted as a, b and c. The $M_s(T)$ curves are given in figure 2. The magnetic unit-cell constant is $2a$ where $a = 3.858$ Å and contains eight Mn atoms. The values of the exchange constants used are $J_1 = -7.9$ K, $J_2 = -6.7$ K, $J_3 = +6$ K.

Sublattice order	x	$A_{\bar{1}}$	$A_{\bar{2}}$	$B_{\bar{2}}$	$B_{\bar{1}}$	$\bar{\mu}$ (μ_B)	$M_s(0)$ (G)	T_c (K)
a	0.5	↑↑↑↑	↑↑↑↑			3.5	570	122
b	0.375	↑↑↑↑	↑↑↑	↓		2.625	424	150
c	0.375	↑↑↑	↑↑	↓↓	↓	0.875	141	148

subscript ($\bar{1}$) relates to crystallographic sites (000) and (aa0) and ($\bar{2}$) to (a00) and (aaa). Figure 2 shows that identical compositions as in (b) and (c) can give very different $M_s(T)$ curves if the distribution of ions on sublattices q_i are different. Since the number of Mn^{4+}–Mn^{3+} nn linkages in the two cases remains nearly the same, the magneto-transport properties are similar. This is also reported by Bahadur *et al* [13]. They find that a sample of $La_{0.6}Er_{0.07}Ca_{0.33}MnO_3$, when prepared by the gel route, has an $M_s(T)$ curve similar to figure 1(c) and its value of $M_s(0)$ at 1 T is 122 G. But when the same composition is synthesized by the ceramic route, the $M_s(T)$ curve is like figure 1(a) and the value of $M_s(0)$ is 610 G. The resistivity curves for the two samples are nearly the same over the temperature range 5 K to 300 K. From figure 2 and table 1, it follows that the gel route sample for $x = 0.375$ has magnetic ordering of the c type and the ceramic route sample has magnetic order of the b type with the magnetization of $B_{\bar{2}}$ reversed due to the double-exchange interaction. This makes the $M_s(T)$ curve close to curve (a) of figure 2. In such cases the magnetization curve can be obtained using a single exchange constant. This is carried out for magnetic order a in table 1 using $J_3 = +12$ K for $H_{ext} = 0$ and 6 T, and shown

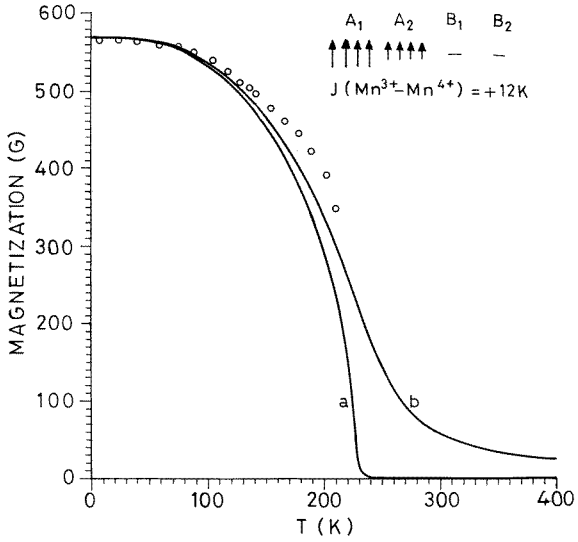

Figure 3. The computer solution for the magnetization curve using equations (51) and (53) (see the text) with the $A_{\bar{1}}$ and $A_{\bar{2}}$ sublattices fully occupied and $J_3 = +12$ K. The external field is zero for curve (a) and 6 T for curve (b). The experimental points are taken from reference [21].

as curves (a) and (b) in figure 3 respectively. The experimental points for $M_s(T)$ obtained for $x = 0.33$ in $La_{1-x}Ca_xMnO_3$ by Pierre *et al* [21] show a reasonably good fit.

As the exchange constants for manganites perovskite are small, application of H_{ext} has a significant effect on the magnetization. In figure 4 we plot the $M_s(T)$ curve for magnetic order a for $H_{ext} = 0$, 1.5 T and 6T. The exchange constant is taken as 6 K which is equal to a Weiss field of 9 T near T_c. We note that T_c is 120 K and is sharply defined when $H_{ext} = 0$. On the application of a field of 6 T, even at 400 K there is a finite value of the magnetization. This accounts for the CMR effect as shown in section 6.

The reported values of T_c depend on the nature of the A-site cation and are 85 K, 260 K and 392 K for $Sm_{0.68}Sr_{0.32}MnO_3$ [28], $La_{0.7}Ca_{0.3}MnO_3$ [29] and $La_{0.7}Sr_{0.3}MnO_3$ [30] respectively. Furthermore, Damay *et al* [28] find that T_c increases linearly with the interpolated cation radius of the A ion in $Sm_{0.56-x}Sr_{0.44-x}Ca_{2x}MnO_3$. As the magnetic order is that of a collinear ferromagnet, a single exchange constant, J_3, can be taken. With the increase in the size of the A cation, the Mn–Mn distance, d, increases. With increase in d, $J^{t_{2g}}$ which opposes ferromagnetic coupling due to the hopping polarons decreases, thereby increasing J_3. If J_3 changes from 5 K to 21 K, the observed variation of T_c can be explained.

6. Magnetoresistance

It follows from equations (39) and (44) that the electron transport in manganites is dependent on the magnetic and bond (atomic) order in the compound. The resistance ratios with and without an external field H can be obtained from equation (44) and are given by

$$\rho_r = \frac{\rho(T,0)}{\rho(T,H)} = \frac{[1+\{1-m^2(t,0)\}\sigma_a^2]}{[1+\{1-m^2(t,H)\}\sigma_a^2]} \exp\left[\frac{U_0}{T}\left\{\xi^2(T,0)-\xi^2(T,H)\right\}\right] \tag{56}$$

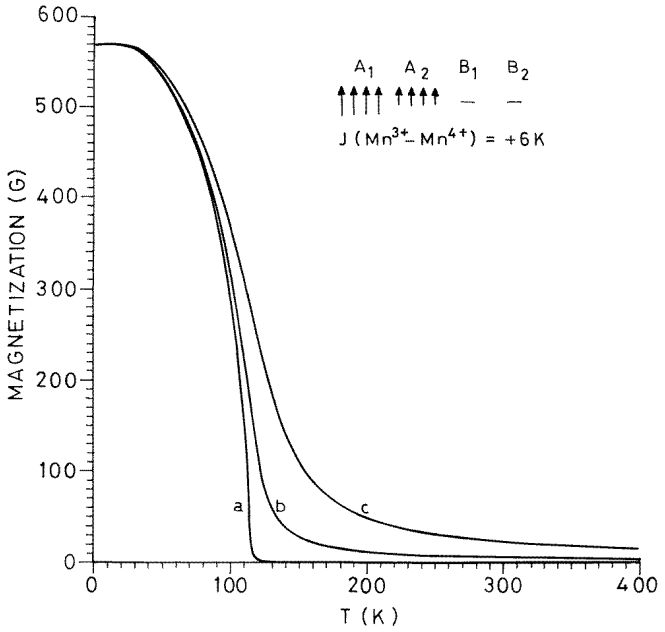

Figure 4. The computer solution for the magnetization curve using equations (51) and (53) (see the text) with the $A_{\vec{1}}$ and $A_{\vec{2}}$ sublattices fully occupied and external field $H_{\rm ext} = 0$ (a), 1.5 T (b) and 6 T (c). The exchange constant J_3 used is 6 K.

or

$$\rho_{\rm r} \simeq \exp\left[\frac{U_0}{T}\left\{\xi^2(T,0) - \xi^2(T,H)\right\}\right]. \tag{56a}$$

In figure 5 a plot of $S_{\rm a}$, $S_{\rm m}$, $\sigma_{\rm a}$ and ξ^2 as functions of $t_{\rm ca}$ is given for $T_{\rm c}/T_{\rm ca} = 0.5$. $S_{\rm m}$ for $H_{\rm ext} = 0$ has been obtained from figure 4 taking $T_{\rm c} = 120$ K and is shown in figure 5. $S_{\rm m}$ for $H_{\rm ext} = 6$ T has also been calculated and used to estimate ξ^2 from equation (41). The values of $\xi^2(0.5, 0)$ and $\xi^2(0.5, 6\ {\rm T})$ are shown by solid curves and that of $\xi^2(0.33, 0)$ by a broken curve in figure 5. $\rho_{\rm r}$ can be readily obtained from figure 5 if U_0 is known.

The magnetoresistance (MR) is defined as

$$\frac{\Delta\rho}{\rho_0} = \frac{\rho(T,H) - \rho(T,0)}{\rho(T,0)} = \frac{1}{\rho_{\rm r}} - 1. \tag{57}$$

Some general comments can be made on the basis of equations (56) and (57) and figure 5 on the dependence of the resistivity and magnetoresistance on temperature and field:

- The activation energy $U_0\xi^2$ at low temperature ($t_{\rm ca} \ll 1$) and high temperature ($t_{\rm ca} \gg 1$) is vanishingly small and peaks in between these limits.
- The peak in ξ^2 occurs near $T = T_{\rm c}$. This peak increases in magnitude as $t_{\rm ca}^{\rm peak}$, where ξ^2 peaks, decreases. Consequently MR increases as $t_{\rm ca}^{\rm peak}$ decreases.
- Under an applied field, a significant reduction in ξ^2 occurs and the peak shifts to higher temperature, enhancing the CMR effect.

All of these features are observed in the CMR effect in manganite perovskites.

In figure 6 the data on $\rho(T)$ for $La_{0.7}Sr_{0.3}MnO_3$ with and without an external field of 6 T obtained by Mahendiran *et al* [30] are compared with equation (44) using the parameters

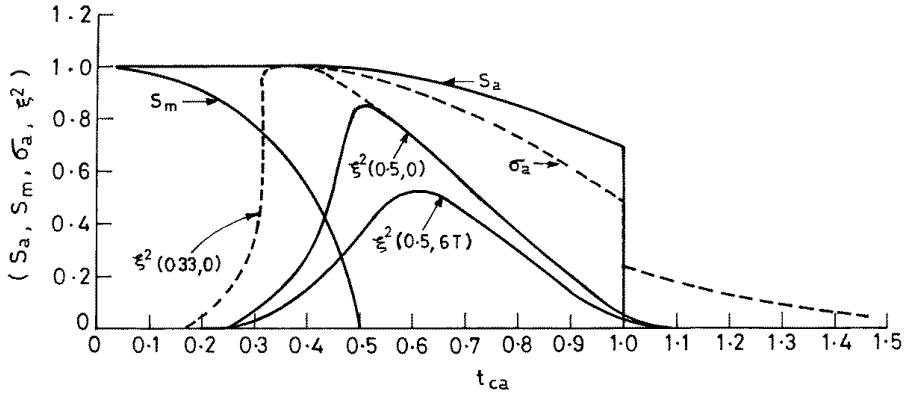

Figure 5. Values of the long-range bond (atomic) order, S_a, long-range magnetic order, S_m, and short-range bond (atomic) order σ_a calculated from equations (48) (see the text) and plotted as functions of $t_{ca} = T/T_{ca}$. The values of S_m have been obtained from figure 4. T_c/T_{ca} has been taken equal to 0.5. ξ^2 has been calculated from equation (41) and plotted as a function of t_{ca}.

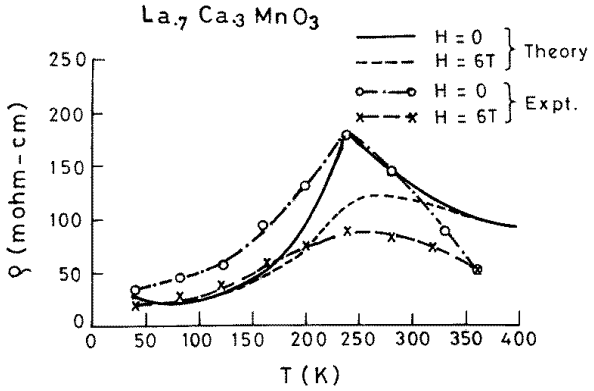

Figure 6. The theoretical curve for $\rho(T)$ for $La_{0.7}Ca_{0.3}MnO_3$ calculated from equation (44) and the parameters A/n, ε_p, U_0, T_c, T_{ca} taken from table 2 is compared with the experimental data from reference [30].

given in table 2. The phonon frequency assumed is 5×10^{12} Hz. For $\rho(T, H)$ only the value of $S_m = m(t)$ changes from that of $\rho(T, 0)$. This is obtained from the computer solution of $M_s(T)$ given in figure 3. For example, $S_m(200, 0) = 0.51$ while $S_m(200, 6\text{ T}) = 0.59$. The general trend of $\rho(T)$ is reproduced both when the field is present and when it is absent.

The largest number of carriers for $La_{0.7}Ca_{0.3}MnO_3$, from table 2, is 2.7×10^{21} cm^{-3}. This gives 0.16 electrons per Mn atom which is half of the theoretical value. There is a large variation of n even for the same composition. This possibly arises due to the polycrystalline nature of the samples.

Damay *et al* [28] have observed $\rho_r = 10^5$ at 75 K for $Sm_{0.58}Sr_{0.3}Ca_{0.12}MnO_3$ at 5 T. They have also reported the $R(T)$ values at $H = 0$ for $Sm_{0.56}Sr_{0.24}Ca_{0.2}MnO_3$. These are compared in figure 7 with the theoretical plot obtained using equation (44) and the values of the parameters given in table 2. The charge density n could not be estimated as the dimensions of the sample were not available.

Table 2. The parameters used to fit the $\rho(T)$ data obtained using equation (44) (see the text). The value of the phonon frequency is taken as $\omega_{ph} = 5 \times 10^{12}$ Hz. The cell constant $a = 3.858$ Å. T_c is obtained from the magnetic data where available. The rest of the parameters are chosen to get the best fit to the $\rho(T)$ curve.

Compound	A/n (10^4 Ω cm K^{-1})	n (10^{20} cm^{-3})	ε_p (K)	U_0 (K)	T_c (K)	T_{ca} (K)	Reference
$La_{0.7}Ca_{0.3}MnO_3$	1.8	4.5	100	250	260	400	[30]
$La_{0.6}Er_{0.07}Ca_{0.33}MnO_3$	1.0	8.1	150	650	180	400	[13]
$La_{0.57}Er_{0.13}Ca_{0.30}MnO_3$	2.0	0.40	70	650	95	300	[13]
$Pr_{0.7}Ca_{0.3}MnO_3$	3.0	2.7	70	650	75	300	[29]
$La_{0.1}Pr_{0.7}Ca_{0.2}MnO_3$	0.8	10.1	70	650	50	300	[29]
$La_{0.35}Pr_{0.35}Ca_{0.3}MnO_3$	0.4	20.2	70	450	150	300	[29]
$La_{0.7}Ca_{0.3}MnO_3$	0.3	27	70	450	250	300	[29]
$La_{0.2}Y_{0.5}Ca_{0.3}MnO_3$	3.0	2.7	600	900	50	400	[29]
$La_{0.35}Y_{0.35}Ca_{0.3}MnO_3$	3.0	2.7	600	650	75	300	[29]
$Sm_{0.56}Sr_{0.24}Ca_{0.2}MnO_3$	—	—	100	1300	95	200	[28]

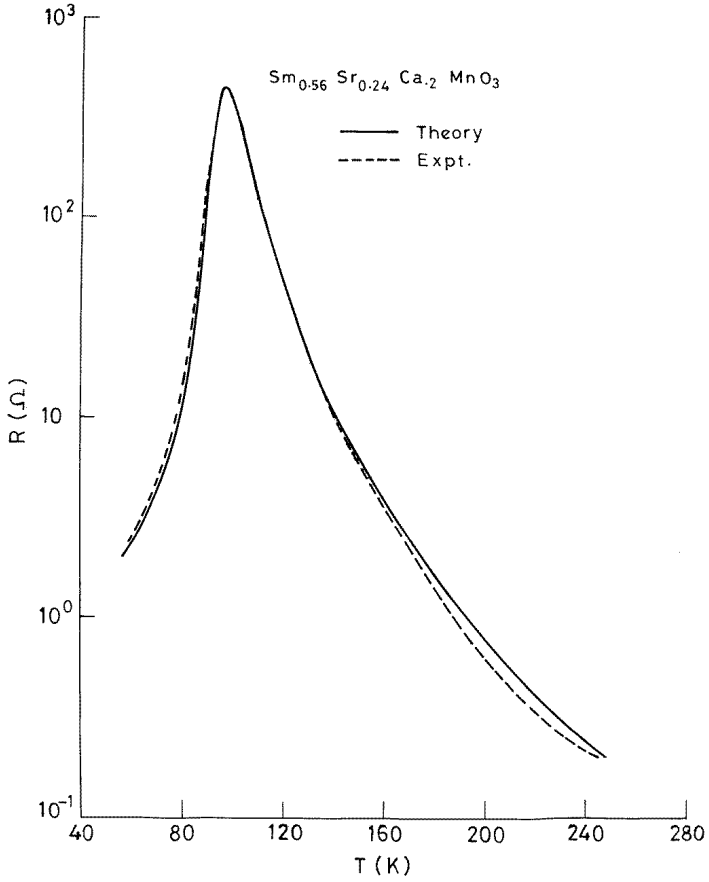

Figure 7. The theoretical curve $\rho(T)$ for $Sm_{0.56}Sr_{0.24}Ca_{0.2}MnO_3$ obtained using equation (44) and the parameters A/n, ε_p, U_0, T_c, T_{ca} taken from table 2 is compared with the experimental values from reference [28].

From equation (56),

$$\ln \rho_r = \frac{U_0}{T}\left[\xi^2(T,0) - \xi^2(T,H)\right]. \tag{58}$$

We obtain from figure 5, with $T_c = 75$ K, $T_{ca} = 150$ K, $U_0 = 1300$ K, $\xi^2(T_c, 0) - \xi^2(T_c, 6\text{ T}) = 0.44$. This gives $\rho_r = 2 \times 10^3$, close to what is observed.

We conclude that for a large CMR effect the binding energy ε_p of the polaron should be small and comparable to the magnetic and bond (atomic) ordering energies. On the other hand the number of phonons in the polaron cloud that determines U_0 should be large.

7. Conclusions

It is shown that the transition from the antiferromagnetic insulating to the ferromagnetic metallic state due to competition between the super-exchange and double exchange expected on the basis of the theory of de Gennes occurs in $Nd_{0.5}Sr_{0.5}MnO_3$. In this system the electrical conduction is by small-polaron hopping, and the relaxation processes for hopping, in both the antiferromagnetic and the ferromagnetic phases, are controlled by the spin–spin scattering. For other perovskite manganites, for a certain concentration of Mn^{4+} ions the magnetic order is determined by the bond ordering and anisotropic super-exchange between Mn^{3+} and Mn^{3+}, and the isotropic super-exchange between Mn^{4+} and Mn^{4+}, as well as by the double-exchange and super-exchange interaction of Mn^{3+}–Mn^{4+} ion pairs. The dc transport for correlated polarons, for which Frank–Condon transitions do not occur, can be described as a diffusion of small polarons such that the mobility satisfies the Einstein relationship. The activation energy for uncorrelated polarons, for which Frank–Condon transitions occur, depends upon the number of phonons in the polaron cloud and so is related to the long- and short-range atomic and magnetic order parameters. This accounts for the presence of colossal magnetoresistance in the system.

Acknowledgments

I am greatly indebted to Professor C N R Rao for introducing me to this fascinating field. I am also grateful to Professor D Bahadur and Professor Shiv Prasad for many stimulating discussions.

References

[1] Jonker G H and Van Santen J H 1950 *Physica* **16** 599
[2] von Helmolt R, Wecker J, Holzapfel B, Schultz L and Samwer K 1993 *Phys. Rev. Lett.* **71** 2331
[3] Asamitsu A, Morimoto Y, Tomioka Y, Arima T and Tokura Y 1995 *Nature* **373** 407
[4] Jin S, Tiefel T H, McCormack M, Fastnacht R A, Ramesh R and Chen L H 1994 *Science* **264** 413
[5] Ishihara S, Inoue J and Maekawa S 1997 *Phys. Rev.* B **55** 8287
[6] Shiina R, Nishitani T and Shiba H 1997 *J. Phys. Soc. Japan* **66** 3159
[7] Wollan E O and Koehler W C 1955 *Phys. Rev.* **100** 545
[8] Goodenough J B 1955 *Phys. Rev.* **100** 564
[9] Zener C 1951 *Phys. Rev.* **82** 403
[10] Anderson P W and Hasegawa H 1955 *Phys. Rev.* **100** 675
[11] de Gennes P G 1960 *Phys. Rev.* **188** 141
[12] Palstra T T M, Ramirez A P, Cheong S W, Zegarski B R, Schiffer P and Zaanen J 1997 *Phys. Rev.* B **56** 5104
[13] Bahadur D, Yewondwossen M, Kozio Z, Foldeaki M and Dunlap R A 1996 *J. Phys.: Condens. Matter* **8** 5235
[14] Holstein T 1959 *Ann. Phys., NY* **8** 343
[15] Reik H G 1972 *Polarons in Ionic Crystals and Polar Semiconductors* ed J T Devreese (Amsterdam: North Holland) pp 679–714

[16] Srinivasan G and Srivastava C M 1981 *Phys. Status Solidi* b **103** 665
[17] Srivastava C M 1991 *Physica* C **176** 481
[18] Anderson P W 1959 *Phys. Rev.* **115** 2
[19] Hiroto K, Kaneko N, Nishizawa A and Endoh E 1996 *J. Phys. Soc. Japan* **65** 3736
[20] Srivastava C M, Srinivasan G and Nanadikar N G 1979 *Phys. Rev.* B **19** 499
[21] Pierre J, Robaut F, Misat S, Strobel P, Nossov A, Ustinov V and Vassilieu V 1996 *Physica* B **225** 214
[22] Caignaert V, Millange F, Hervieu M, Suard E and Raveau B 1996 *Solid State Commun.* **99** 173
[23] Srivastava C M 1998 *Pramana* **50** 11
[24] Mott N F 1968 *J. Non-Cryst. Solids* **1** 1
Austin I G and Mott N F 1969 *Adv. Phys.* **81** 41
Mott N F and Davis E A 1979 *Electronic Processes in Non-Crystalline Materials* 2nd edn (Oxford: Clarendon)
[25] Muto T, Eguchi T and Shibuya M 1948 *J. Phys. Soc. Japan* **3** 277
Muto T and Tazagi Y 1955 *Solid State Physics* vol 1, ed F Seitz and D Turnbull (New York: Academic) p 193
[26] Fisher M E and Langer J S 1968 *Phys. Rev. Lett.* **20** 665
[27] Nix F C and Shockley W 1938 *Rev. Mod. Phys.* **10** 1
[28] Damay F, Nguyen N, Maignan A, Hervieu M and Raveau B 1996 *Solid State Commun.* **98** 997
[29] Mahendiran R, Mahesh R, Raychaudhuri A K and Rao C N R 1996 *Solid State Commun.* **99** 149
[30] Mahendiran R, Mahesh R, Raychaudhuri A K and Rao C N R 1995 *Solid State Commun.* **94** 515